On the performance of a limited area model for quantitative precipitation forecast over Calabria

S. Federico([1]), E. Avolio([2]), C. Bellecci([1])([2]) and M. Colacino([3])

([1]) *CRATI s.c.r.l. c/o Università della Calabria - 87036 Rende (CS), Italy*
([2]) *INFM-Università di Roma "Tor Vergata", Dept. STFE - Via di Tor Vergata 00133 Rome, Italy*
([3]) *CNR-IFA - Via del Fosso del Cavaliere 100, 00133 Rome, Italy*

Summary. — At Crati Scrl an operational version of RAMS 4.3 (Regional Atmospheric Modeling System), with a son grid over Calabria, was implemented in January 2001. This paper aims to give a first assessment of model performances for quantitative precipitation forecast (QPF). In particular two issues of weather forecast are discussed. First problem refers to effects introduced by enhanced resolution over Calabria, using a 6 km resolution grid nested in a 30 km parent grid. Second issue discusses forecast deterioration with increasing forecast time. To cope with these problems, two sets of integrations are discussed using two different model configurations. Differences between configurations are only due to model resolutions. Integrations are performed daily for six months. Each integration starts at 12 UTC and lasts for 60 h, with 12 h spin-up time. ECMWF 12 UTC analysis and following forecast are used as initial and dynamic boundary conditions. Models performances are evaluated computing scores by comparing model outputs with raingauges data coming from Calabria regional network. Results show better performances of finer-grid resolution compared to the coarser one and confirms the usefulness of enhanced resolution over complex terrain. In addition, performances decrease with increasing forecast time with first integration day performing better than second forecast day but differences are not statistically significant at 5% level.

PACS `92.60.Jq` – Water in the atmosphere (humidity, clouds, evaporation, precipitation).
PACS `93.85.+q` – Instrumentation and techniques for geophysical research.

1. – Introduction

The aim of this paper is to give a first assessment of RAMS accuracy in quantitative precipitation forecast (QPF) over Calabria. Improving QPF is one of the most desired aspects in numerical weather prediction to the general community.
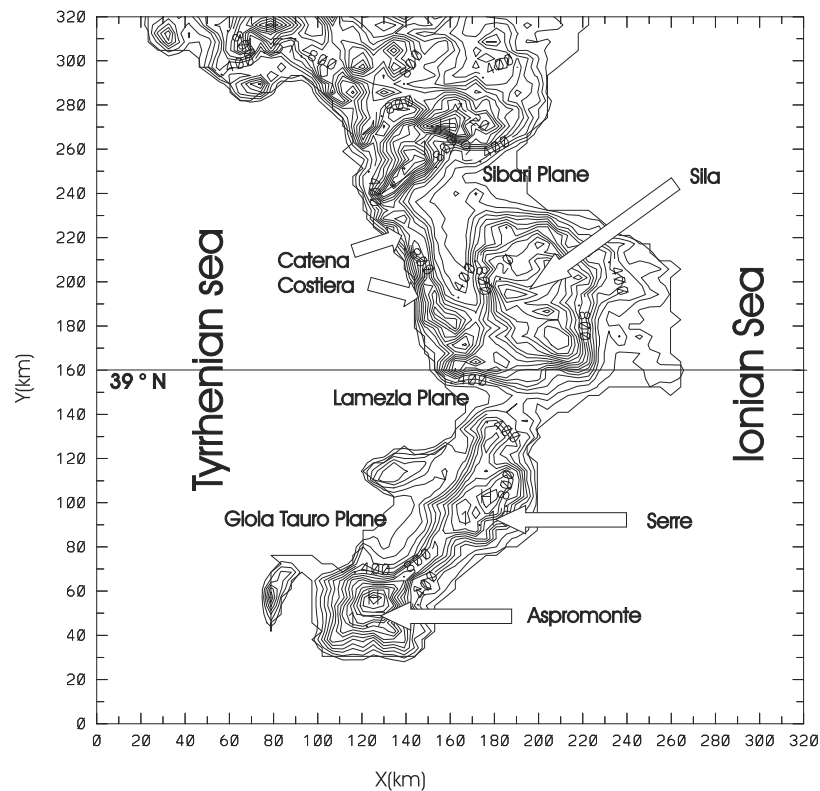
Fig. 1. – Topography of Calabria averaged over 10 km^2. Main features are also reported.

Unfortunately precipitation is a difficult field to predict quantitatively. There are several reasons for that. First of all the process depends on several factors as temperature, humidity, winds in highly non-linear ways. Another complication is introduced by variable physiography, *i.e.* surface features such as topography, land water boundaries, vegetation and soil parameters. All those features are important in Calabria, fig. 1, and, in particular, the presence of mountains may act to enhance rainfall by several mechanism including low-level convergence associated with flow deflection around the topography [1-3] and terrain-triggered convection [4].

Among others, model resolution over complex terrain is claimed as an important factor to better represent small-scale variations not considered in global-scale models [5]. This is the first point investigated in this paper.

Another important aspect of QPF is the decrease of performances with increasing forecast time. As pointed out by Lorenz [6, 7] the atmosphere is a chaotic system and even an infinitesimally small perturbation introduced into the atmosphere at a given time will result in an increasingly large change in the evolution of the system so that, after two or three weeks, trajectories of the perturbed and original atmosphere would be completely different. Stated in other terms, arbitrarly small initial perturbations evolve in large differences with time. To cope with this problem, different techinques, as the ensemble forecasting [8,9], have been developed. However, the main point is that even in a perfect model, due to analysis errors the skill of forecasts would degrade to zero with

increasing forecast time. Analysis errors can be due to lack of complete coverage, errors in measurements, errors in first guess and to the approximation of analysis technique. In addition model errors degrade performances with increasing forecast time and errors are introduced by both physical and numerical parameterizations. So, all these factors determine a decrease in model skills with increasing forecast time and this is the second point investigated in this paper.

More precisely, with respect to quantitative precipitation forecast, two questions are discussed: is the resolution enhancement a benefit for rainfall forecast over Calabria? How do performances deteriorate with increasing forecast time for the first two integration days?

To answer the first question, we analyze RAMS model in two different forecast configurations for a six month period, from 1 November 2000 to 30 April 2001; the first configuration uses only one grid, while the second set-up uses two grids. In both cases the first grid has 30 km resolution. In the second configuration case we add to the first configuration grid a nested grid with 6 km spacing. Hereafter we will refer to the two configurations introduced above as CC (Coarse Configuration) and FC (Fine Configuration).

To answer the second question, we adopt the following technique. Each day of the six month period, *i.e.* from 1 November 2000 to 30 April 2001, we perform a 60 h forecast starting from 12 UTC ECMWF analysis/forecast cycle. First 12 h are spin-up time while the remaining 48 h are the actual forecast. This time period is divided into two 24 h verification periods, 0-24 h and 24-48 h. First 24 h are the forecast for the first integration day, last 24 h are forecast for the second integration day. These two forecasts will be also referred as 1D forecast and 2D forecast.

In summary, in order to, at least partially, answer the questions raised above we show results for six month integrations, each lasting 60 h, using two model configurations, CC and FC. Differences between CC and FC will be used to assess the effects of enhanced resolution in quantitative precipitation forecast over Calabria. Comparison between first and second day FC forecasts is used to assess performance degradation between first and second forecast days.

Forecasts are compared each other using scores computed comparing models outputs with raingauge measurements available from the ARPACAL (Calabria regional agency for environmental protection) network. Measurements are available at 36 locations and are shown in fig. 2. Data refer to daily cumulated rainfall. Differences significance between model scores is assessed by the application of a statistical test proposed by Hamill [10,11].

2. – Model set-up

The following is a brief description of the model set-up including options selected. For details on RAMS model the reader should refer to Pielke *et al.* and Cotton *et al.* [12,13]. Grids configuration is shown in fig. 3. For CC configuration we use first grid only, with 30 km grid spacing. FC configuration uses also the second grid, nested in the CC grid, by a two way interacting grid procedure with a 6 km grid spacing [14] and a nesting ratio of 5. Communication from the parent to the nested grid is accomplished immediately following a timestep on the parent grid which updates prognostic fields. Nested-grid timestep is, usually, less than the parent grid time step, so, after the communication, the nested grid is updated in a series of smaller time steps until its integration time equals the parent grid simulation time. At this time, the reverse communication is accomplished.
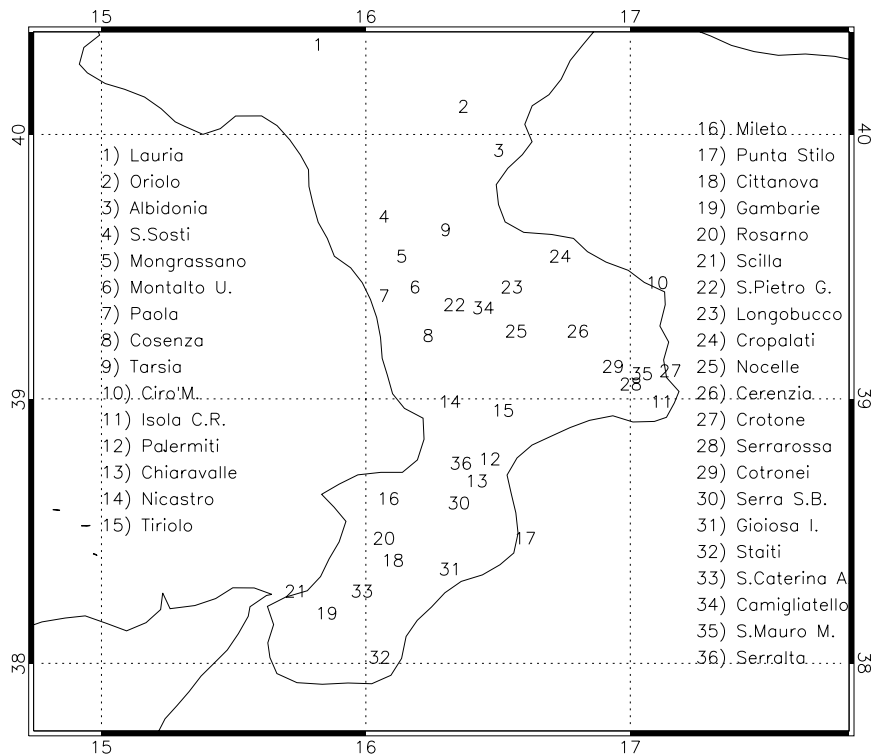
Fig. 2. – Station subset of ARPACAL network used to compute scores.

Twenty five vertical levels, up to 12500 m in the terrain following coordinate system, are used in simulations. Levels are not equally spaced: within the PBL (Planetary Boundary Layer) layers run about 50–200 m tick, while in the middle and upper troposphere they are 1000 m tick.

The parameterization of the surface-atmosphere diabatic processes is described in Walko [15]. Non-convective precipitation is calculated from explicit prognostic equations for eight hydrometeors: total water, rain, pristine, cloud particles, ice, snow, hail and aggregates. A generalized gamma function is used to describe hydrometeors size distribution [16]. Convective precipitation is parameterized following Molinari and Corsetti [17] who proposed a simplified form of the Kuo scheme that accounts for updrafts and downdrafts. Sea surface temperature (SST) is a function of the position but, during the simulation, it is held constant in time. The dataset currently used in RAMS contains one degree resolution global monthly climatological values of SST.

Initial conditions are provided by 12 UTC ECMWF analysis, while dynamic boundary conditions are interpolated to RAMS grids by the following ECMWF forecast. The horizontal resolution of the ECMWF analysis is one degree. Simulations duration is 60 h. First 12 h are used as spin-up time so 48 hours are available for discussion. This time window corresponds to a 2 days forecast, the 1D and 2D forecast.
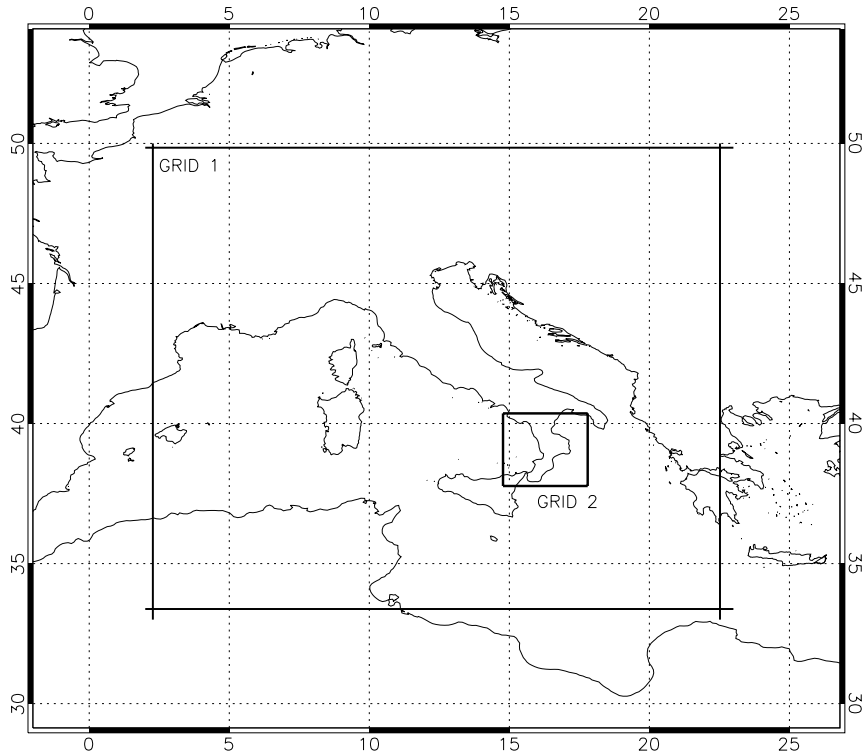
Fig. 3. – Grids used to verify forecasts. First grid is used in both CC and FC forecasts and has 30 km grid spacing. Second grid is used for FC forecast, its spacing is 6 km.

3. – Verification methodology and data

3˙1. *Scores*. – In this subsection we quickly introduce scores used in this paper. A thorough review can be found in Hamill and Accadia *et al.* [10, 11].

Scores are useful for evaluating deterministic gridded precipitation forecasts as these reported in this paper. They are generated from contingency tables, as the one shown in table I, as follows. Precipitation space is divided in four, mutually exclusive and exhaustive sets: *hits* (hereafter indicated also by a) represent the number of locations in which both model and measurement are greater than or equal to a threshold; *false alarms* (hereafter indicated also by b) represent the number of locations where the model is above a threshold while the measure is under the same threshold; *misses* (hereafter indicated also by c) represent the number of locations where the measure is above a threshold while the forecast value is under the same threshold; *correct no forecasts* (hereafter indicated also by d) represent the number of locations where the model and measures are both under the threshold.

Starting from the contingency table we can define the BIA:

$$\mathrm{BIA} = \frac{a+b}{a+c};$$

BIA measures if the model overforecasts or underforecasts precipitation over an area.

TABLE I. – *Contingency table of possible events.*

		Observed	
		Yes	No
	Yes	a	b
Forecast	No	c	d

If BIA > 1, the model overestimates the precipitation area, while if BIA < 1 the model underestimates this area. For a perfect forecast BIA $= 1$.

Another important score, the most widely used, is Equitable Threat Score (ETS) defined as

$$\text{ETS} = \frac{a - a_{\text{r}}}{a + b + c - a_{\text{r}}},$$

where a_{r} is the expected number of correct forecasts above the threshold in a random forecast where forecast occurrence/non occurrence is independent of observation/non observations. It is defined as

$$a_{\text{r}} = \frac{(a + b)(a + c)}{a + b + c + d}.$$

For a perfect forecast ETS is equal to 1, while it is less than or equal to zero for a useless forecast.

Another score discussed in this paper is the Hanssen-Kuipers one defined as

$$\text{HK} = \frac{ad - bc}{(a + c)(b + d)}.$$

Unlike ETS this score emphasizes forecast and non-forecast events. Indeed, it can be written as the difference between the probability of detection (POD) and false alarm rate (F) [18]:

$$\text{HK} = \text{POD} - F = \frac{a}{(a + c)} - \frac{b}{(b + d)};$$

POD is the number of the frequency of yes forecast when the event occurs, while F is the frequency of yes forecast when the event does not occur.

3.2. *Forecast and verification data*. – To verify forecasts, we use data from a subset of ARPACAL network (fig. 2). The network considered has 36 stations dislocated in Calabria. For these stations, on every day of the verification period, a contingency table is computed. Model precipitation forecast is cumulated over 24 h too, excluding first 12 h of spin-up time as discussed in sect. **1**. Each observation is assigned to the nearest grid point and the observed grid point precipitation is the average for all observations associated with the grid point.

To compare forecasts coming from different grid configurations, or from the same grid for different integration days we use a hypothesis test developed by Hamill [10] that is

based on resampling. The null hypothesis of the resampling tests is that differences in scores of competitor forecasts, computed from a sum of daily contingency table samples over all the case days, are zero. If S is the generic score (introduced in previous subsection), we have

$$H_0 : S_1 - S_2 = 0$$

and the alternative hypothesis is

$$H_1 : S_1 - S_2 \neq 0\,,$$

where 1 and 2 are the competitor forecasts. Statistics S_1 and S_2 are scores computed from the summation of contingency tables over the whole period considered, *i.e.* if $\boldsymbol{x}_{i,j}$ is the contingency table for model i and day j,

$$x_{i,j} = (a,b,c,d)_{i,j}\,, \qquad i = 1,2\,, \quad j = 1,....,n\,,$$

the test statistic S will be computed from the summation

$$S_1 \qquad (a,b,c,d)_1 = \sum_{k=1}^{n} x_{1,k}$$

for model 1 and from the summation

$$S_2 \qquad (a,b,c,d)_2 = \sum_{k=1}^{n} x_{2,k}$$

for model 2. n is the total forecasts number and, in our case, it is 180.

Resampled test statistics consistent with the null hypothesis are generated after randomly choosing either one or the other model on each day and summing contingency table elements. In this way we obtain the statistics distributions that are used to accept or discard the null hypothesis at the test level α. In this paper we use a two-sided test with significant level of $\alpha = 0.05$. To calculate the resampled test statistics, we generate n random samples of an integer I that takes on the value 1 or 2. Resampled statistics is computed from the following contingency table summations:

$$S_1^* : \qquad (a,b,c,d)_1^* = \sum_{k=1}^{n} x_{I_k,k}$$

and

$$S_2^* : \qquad (a,b,c,d)_2^* = \sum_{k=1}^{n} x_{3-I_k,k}\,.$$

This process is repeated 10000 times to build the null distribution. The difference between S_1 and S_2 is finally tested by determining the location of $(S_1 - S_2)$ in the resampled distribution $(S_1^* - S_2^*)$. Formally, we compute $\hat{t}_L$ and $\hat{t}_U$ that represent the

$\alpha/2$ percentile and $1 - \alpha/2$ percentile of the null distribution $(S_1^* - S_2^*)$. Then the null hypothesis H_0 is rejected, at the confidence level α, if

$$(S_1 - S_2) < \hat{t}_L \qquad \text{or} \qquad (S_1 - S_2) > \hat{t}_U \,.$$

4. – Results

In this paper we consider the following rainfall in a day: 1 mm, 5 mm, 10 mm, 20 mm, 30 mm, 40 mm, 50 mm. They represent a good compromise between precipitation quantity falling in a day over Calabria and the intrinsic field variability [19].

First of all we discuss the effects on QPF determined by adding a nested grid to simulations. Results for BIA, ETS, HK, POD and F are presented for the first forecast day in figs. 4a–e. Each figure has three curves. Dot-dashed line is the score for CC configuration, that has one grid only, solid line is the score of the second grid of FC configuration, dotted line is the FC first-grid score. Error bars, reported for dotted line, represent values of $\hat{t}_L$ and $\hat{t}_U$ of statistical test involving first grid of FC and CC grid, at 5% level. These two grids are identical in terms of lattice location in space, so comparison is straightforward. Indeed, another point that should be emphasized is that actual values of scores depend on the spatial smoothness of verification analysis. With station reports simply box averaged, analysis smoothness will depend on the volume of data available per verification box. We compare the first FC grid with CC because the volume of data is the same for both grids. However, performances for the second FC grid are shown because there are few remarks to note. In addition, due to its better behaviour, the second grid of FC will be used in the assessment of forecast deterioration with increasing forecast time.

Figure 4a shows that BIA for CC configuration is at every threshold less than BIA for both grids of FC configuration. Differences are statistically significant at 5% level for all precipitation values. The use of a nested grid in FC forecast enhances precipitation on the first one by the two-way interactive procedure [14]. This results in a general overestimation of BIA for the first grid of FC. At high thresholds, let us say higher than 20 mm, BIA low values for CC configuration are obviously due to the poor resolution of this forecast that underestimates mountain heights and orographic uplift that is an important mechanism for precipitation enhancement. At 50 mm, in particular, BIA is zero for CC forecast.

At lower thresholds ($\leqslant 20$ mm) rainfall triggering mechanisms are fundamentals. A closer inspection of model outputs reveals that light precipitation events are sometimes missed by CC forecast just because local physiographic features are not enough represented in the model. These same precipitation events are, at least partially, represented by FC (*i.e.* for FC simulations *hits* are not equal to zero). As large scale forcing is the same for both FC and CC forecasts, it follows that, in these cases, local orographic features are able to trigger precipitation in FC forecast due to the enhanced model resolution. As a consequence, at lower thresholds, BIA is underestimated by CC forecast, while it is slightly overestimated by FC. BIA results show that local orography is fundamental at all rain amounts considered in this paper. This should be considered in weather-related activities that do not necessarily involve large precipitation amounts.

ETS score is shown in fig. 4b. FC forecast performs better at all thresholds. Differences are statistically significant at 5% level, if we exclude 1 mm rainfall. Also in this case, for 50 mm/day rainfall, ETS score is zero and CC forecast is not useful for thresholds greater than 20 mm. FC first-grid forecast has larger ETS values than CC
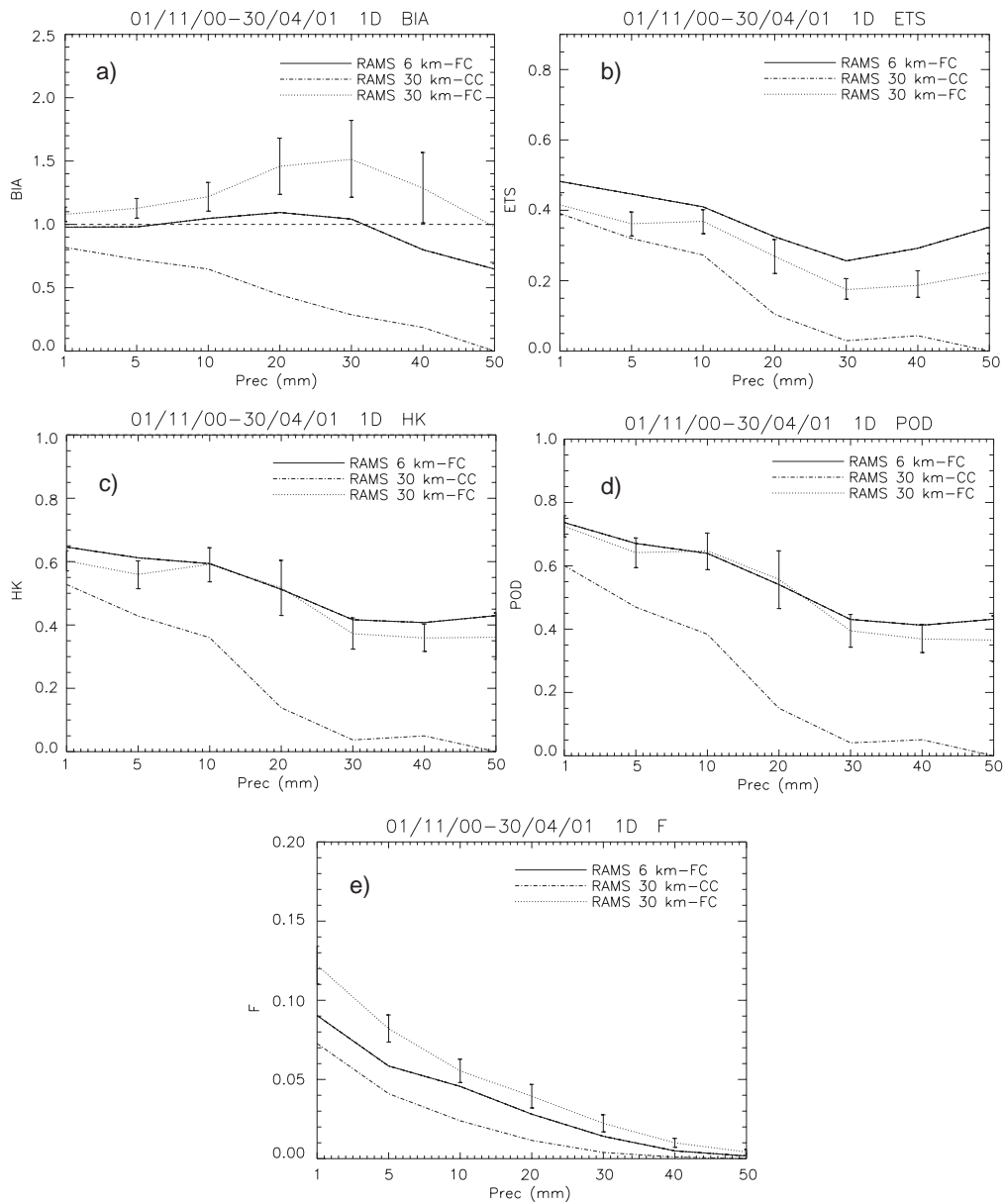
Fig. 4. – BIA (a), ETS (b), HK (c), POD (d) and *F* (e) scores for the first forecast day. Solid line is for FC second grid, dot-dashed line is for CC forecast, dotted line is for FC first grid. Error bars are computed according to Hamill test (see text).

but lower than its nested grid. However, it maintains usefulness at all threshold, being well above the zero value. From fig. 4b there follows the ability of the nested grid to better reproduce precipitation spots, as a consequence of a finer representation of Calabria physiographic features.

Figure 4c shows HK for 1D forecast. Also in this case FC model performs better, in a statistical significant way at 5% level, for all thresholds. This is due to a greater POD of FC compared to CC case and shows again the importance of local physiographic features in determining precipitation over Calabria. Results for POD are shown in fig. 4d. There are large differences between CC and FC forecasts.

F score is reported in fig. 4e. Also in this case results are statistically significant at all thresholds, however for this score CC forecast "performs better". False alarm rate, *i.e.* the number of yes forecast when the event did not occur, is lower for CC forecast than for FC. This result, however, is tricky because it is due to the absence of yes forecast in CC. As an example, F ratio at 50 mm threshold is perfect, *i.e.* zero, just because CC forecast never reached this rainfall in a day, while raingauge data reached this threshold for about 1.5% of rain measurements. So, for this threshold, CC forecast is not perfect, it is useless.

Figure 5 shows scores for 2D forecast. Curves are as in fig. 4. Figure 5a shows a general increase of BIA, compared to first forecast day, for both forecast configurations. In this case, CC forecast BIA is different from zero for all thresholds. CC and FC are again different, at 5% level, at all thresholds with FC performing better.

ETS confirms results obtained for first forecast day and FC performs better at all thresholds, even if differences are not statistically significant at 1 mm and 5 mm thresholds. ETS is less than zero for the coarser model configuration at 50 mm threshold and confirms that CC model is useless at high precipitation thresholds, at least for the integration period considered in this paper. HK score, fig. 5c, confirms previous results. It is greater for FC forecast due to the greater POD (fig. 5d) that is a consequence of better physiografic representation of FC model compared to CC. F score shows larger values for more resolved model compared to CC, however same discussion made for first day applies. In conclusion, the use of a son grid over Calabria, having 6 km resolution, produces better model performances not only for large rain forecast but also at lower thresholds that are important for several humans activities.

As shown in figs. 4 and 5, FC nested grid has best ETS values so we use results of second FC grid to examine forecast performance deterioration with increasing simulation time.

Figures 6a-e report scores for the second FC grid; solid line refers to first forecast day, 1D, dot-dashed line shows second day forecast scores, 2D. Error bars represent values of $\hat{t}_L$ and $\hat{t}_U$ of statistical test involving 1D and 2D forecasts for FC second grid, at 5% level.

BIA shows better performances of 1D forecast up to 30 mm threshold. At higher threshold 2D forecast performs better. However, differences are never statistically significant at 5% level.

Figure 6b shows ETS for first and second day forecasts. In this case 1D forecast performs better at all thresholds but differences are statistically significant only for 20 mm thresholds. Nevertheless, ETS shows signals of forecast deterioration with increasing forecast time.

Inspection of contingency tables reveals that, compared to 1D forecast, 2D forecast has an increase of *false alarms* (*b*) and a decrease of *correct no forecasts* (*d*) with minor changes on *hits* (*a*) and *misses* (*c*). As a consequence BIA values for 2D forecast are
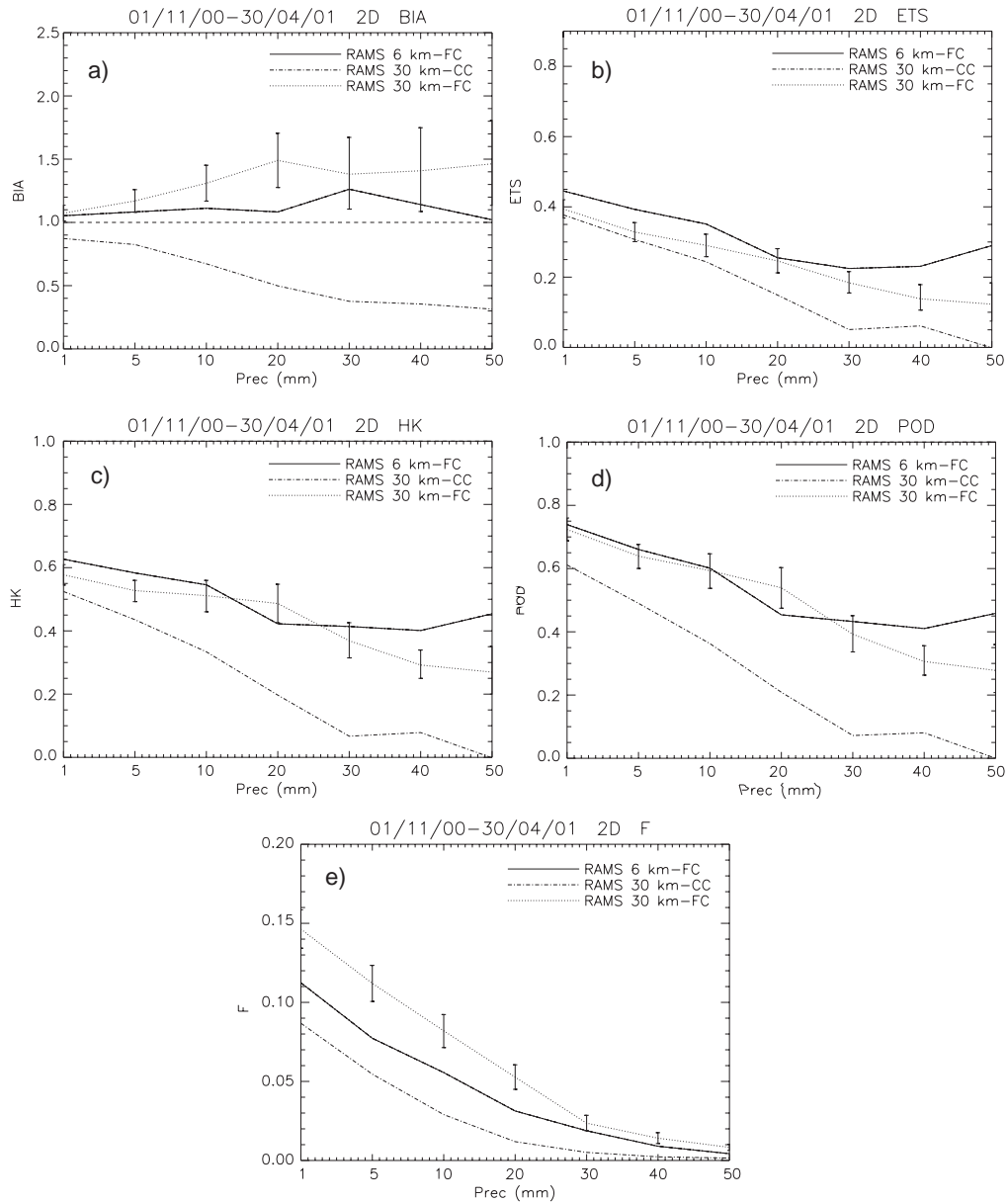
Fig. 5. – As in fig. 4, but for the second forecast day.

higher than 1D forecast because the model is more able to represent the precipitation area but correct locations are missed. This explains why, despite the larger BIA values, ETS is lower for 2D forecast at all thresholds.

Another consequence of these differences of contingency tables between 1D and 2D forecasts is that POD values at higher thresholds are similar (fig. 6d). Indeed POD values depend only on *hits* (*a*) and *misses* (*c*) that do not show large variations between
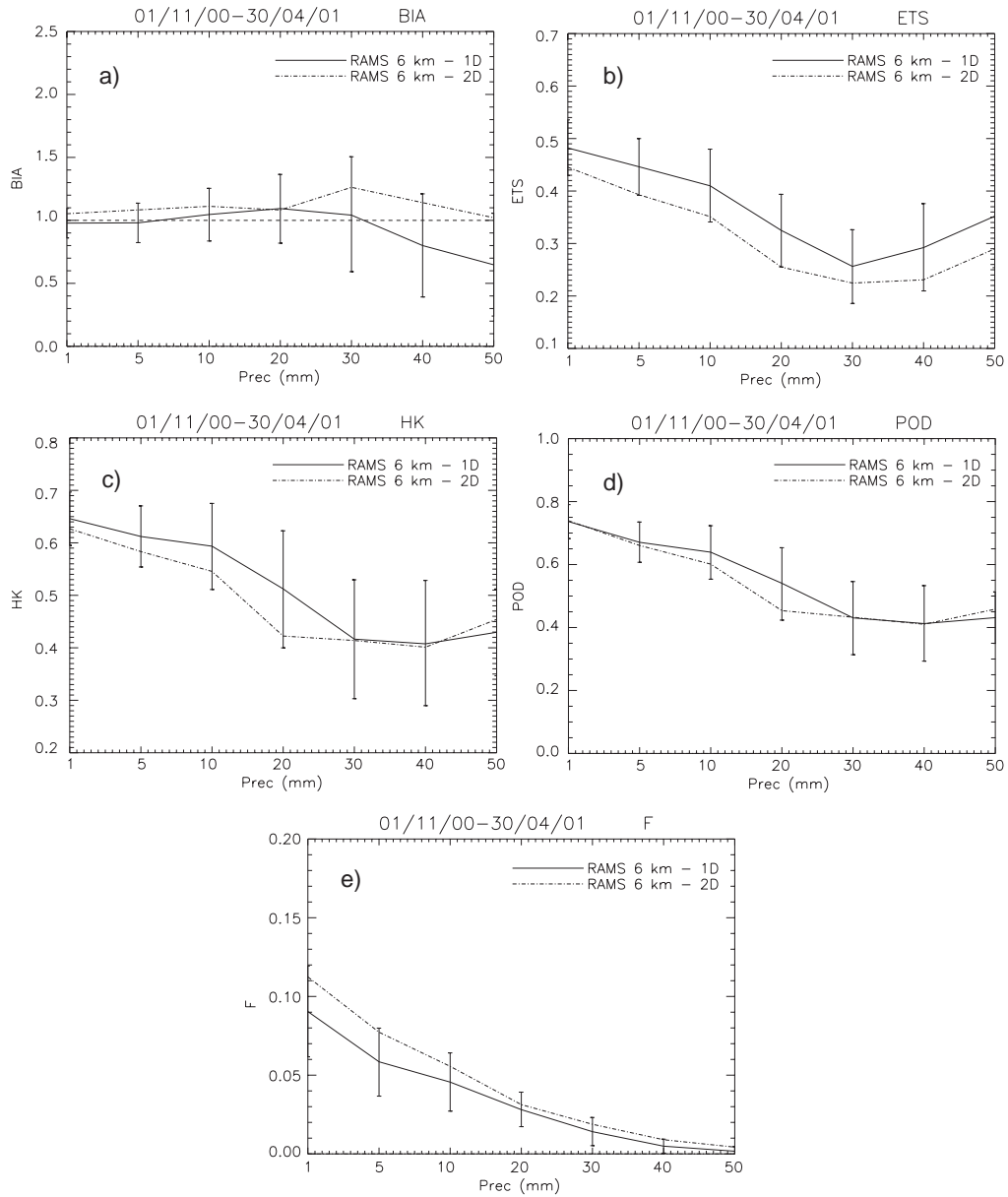
Fig. 6. – BIA (a), ETS (b), HK (c), POD (d) and F (e) scores for the first and second forecast days. Curves refer to second grid of FC forecast. Solid line is for first forecast day, dot-dashed line is for second forecast day. Error bars are computed according to Hamill test (see text).

1D and 2D forecasts. At the same time, F score is strongly affected by large values of d, *i.e.* correct no forecast, due to typical values of rainfall over Calabria [19]. Indeed values of d are at least one order of magnitude greater than other terms in contingency tables. As a consequence F values (fig. 6e) are larger for 2D forecast compared to 1D, but they are a order of magnitude less than POD values. This results in comparable values of HK (fig. 6d) for competitor models at thresholds greater or equal to 30 mm. Considering variations in contingency tables stated above and scores expressions reported in previous section, it follows that ETS and BIA are more sensible to these changes compared to HK, while POD is not dependent on b and d. It should be considered, in addition, that statistical samples are reduced at higher thresholds because model outputs and measurements above a threshold decrease for increasing rain values. As a consequence, a longer period of analysis is underway to confirm this issue.

In summary, with respect to 1D and 2D forecasts, we can divide thresholds in two groups: lower thresholds and higher thresholds. The former contains values lower or equal to 20 mm, the latter contains values larger than 20 mm. Figure 6 shows better results of 1D forecast for ETS at all thresholds and this suggests model performances deterioration with increasing forecast time, however differences for HK and POD values are not always evident.

Even if a direct comparison between first and second grids of FC forecast cannot be made, due to the verification methodology adopted in this paper, it is interesting to give few brief remarks. ETS shows clearly that fine grid is more able to better represent rainfall locations due its higher resolution. Nevertheless differences in HK and POD are not evident at all thresholds. As for the case of 1D and 2D forecasts comparison, differences between first and second FC grids contingency tables involve mainly changes of *false alarms* (b) and *correct no forecasts* (d). In particular first grid has larger values of b and lower values of d. d values are at least one order or magnitude less than a, b and c. As discussed above, ETS and BIA are more sensible to these changes in contingency tables compared to HK, while POD is not dependent on b and d values.

5. – Conclusions

In this paper we investigated performances of RAMS model for quantitative precipitation forecast over Calabria. Two different model configurations were tested in order to, at least partially, assess two important aspects of regional weather forecast:

1) benefits of using 6 km grid spacing compared to 30 km grid resolution;

2) performance deterioration with increasing forecast time.

Conclusions are as follows.

– The use of a nested grid over Calabria is useful at all precipitation thresholds used in this paper. Indeed resolution enhancement produces a better representation of physiographic features that results in better performances not only for large precipitation events but also for light rain. Better performances of fine-resolution forecast are evident for both integration days and performances are statistically significant at 5% rejection level.

– Differences between first and second forecast days show better model performances for the first day. Differences between competitor models are not statistically significant at 5% level, with only one exception for ETS. Changes between 1D and

2D forecasts are mainly due to *false alarms* and *correct no forecasts* in contingency tables. In particular, RAMS model has larger *b* values and lower *d* values for the second integration day. While statistical population is large for thresholds $\leqslant 30$ mm, a longer analysis is underway to better assess this issue for high precipitation values in order to obtain more populated samples.

$$* * *$$

REFERENCES

[1] BUZZI A., TARTAGLIONE N. and MALGUZZI P., *Mon. Weather Rev.*, **126** (1998) 2369.
[2] ROTUNNO R. and FERRETTI R., *J. Atmos. Sci.*, **58** (2001) 1732.
[3] SMITH R. B., *The influence of mountains on the atmosphere*, in *Advances in Geophysics*, Vol. **21** (Academic Press) 1979, pp. 87-230.
[4] FEDERICO S., BELLECCI C. and COLACINO M., *Nuovo Cimento C*, **26** (2003) 7.
[5] GAUDET B. and COTTON W. R., *Weather Forecasting*, **13** (1998) 966.
[6] LORENZ E. N., *J. Atmos. Sci.*, **20** (1963) 130.
[7] LORENZ E. N., *Tellus*, **17** (1965) 321.
[8] MOLTENI F. and PALMER T. N., *Q. J. R. Meteorol. Soc.*, **119** (1992) 269.
[9] TOTH Z. and KALNAY E., *Bull. Am. Meteorol. Soc.*, **74** (1993) 2317.
[10] HAMILL T. M., *Weather Forecasting*, **14** (1999) 155.
[11] ACCADIA C., CASAIOLI M., MARIANI S., LAVAGNINI A., SPERANZA A., DE VENERE A., INGHILESI R., FERRETTI R., PAOLUCCI T., CESARI D., PATRUNO P., BONI G., BOVO S. and CREMONINI R., *Nuovo Cimento C*, **26** (2003) 61.
[12] PIELKE R. A., COTTON W. R., WALKO R. L., TREMBACK C. J., LYONS W. A., GRASSO L. D., NICHOLLS M. E., MURRAN M. D., WESLEY D. A., LEE T. H. and COPELAND J. H., *Meteorol. Atmos. Phys.*, **49** (1992) 69.
[13] COTTON W. R., PIELKE R. A. SR., WALKO R. L., LISTON G. E., TREMBACK C. J., JIANG H., McANELLY R. L., HARRINGTON J. Y., NICHOLLS M. E., CARRIO G. G. and McFADDEN J. P., *Meteorol. Atmos. Phys.*, **82** (2003) 5.
[14] WALKO R. L., TREMBACK C. J., PIELKE R. A. and COTTON W. R., *J. Appl. Meteorol.*, **34** (1994) 994.
[15] WALKO R. L., BAND L. E., BARON J., KITTEL T. G., LAMMERS R., LEE T. J., OJIMA D., PIELKE R. A. SR., TAYLOR C., TAGUE C., TREMBACK C. J. and VIDALE P. L., *J. Appl. Meteorol.*, **39** (2000) 931.
[16] WALKO R. L., COTTON W. R., MEYERS M. P. and HARRINGTON J. Y., *Atmos. Res.*, **38** (1995) 29.
[17] MOLINARI J. and CORSETTI T., *Mon. Weather Rev.*, **113** (1985) 485.
[18] STEPHENSON D. B., *Weather Forecasting*, **15** (2000) 221.
[19] COLACINO M., CONTE M. and PIERVITALI E., *Elementi di climatologia della Calabria*, IFA-CNR (1997).